Information Thermodynamics of Turing Patterns

Gianmaria Falasco, Riccardo Rao, and Massimiliano Esposito
Complex Systems and Statistical Mechanics, Physics and Materials Science Research Unit, University of Luxembourg, L-1511 Luxembourg

(Received 14 March 2018; revised manuscript received 15 June 2018; published 4 September 2018)

We set up a rigorous thermodynamic description of reaction-diffusion systems driven out of equilibrium by time-dependent space-distributed chemostats. Building on the assumption of local equilibrium, nonequilibrium thermodynamic potentials are constructed exploiting the symmetries of the chemical network topology. It is shown that the canonical (resp. semigrand canonical) nonequilibrium free energy works as a Lyapunov function in the relaxation to equilibrium of a closed (resp. open) system, and its variation provides the minimum amount of work needed to manipulate the species concentrations. The theory is used to study analytically the Turing pattern formation in a prototypical reaction-diffusion system, the one-dimensional Brusselator model, and to classify it as a genuine thermodynamic nonequilibrium phase transition.

DOI: 10.1103/PhysRevLett.121.108301

Introduction.—Reaction-diffusion systems (RDSs) are ubiquitous in nature. When nonlinear feedback effects within the chemical reactions are locally destabilized by diffusion, complex spatiotemporal phenomena emerge. These latter ranging from stationary Turing patterns [1,2] to traveling waves [3,4] play a critical role in the aggregation and structuring of hard matter [5] as well as living systems [6]. In biology, striking examples are embryogenesis determined by the prepatterning of morphogens [7–9] and cellular rhythms regulated by calcium waves [10,11].

Nonequilibrium conditions consisting in a continual influx of chemicals and energy are required to create and maintain these dissipative structures. Since the original work of Prigogine and Nicolis [12,13], which made clear how order can emerge spontaneously at the expense of continuous dissipation, much work has been dedicated to better understanding the chaotic and nonequilibrium dynamics of RDSs [14]. Most of it has focused on searching for general extremum principles, e.g., in selecting the relative stability of competing patterns [15]. Nevertheless, a complete framework is still lacking that models RDSs as proper thermodynamic systems in contact with nonequilibrium chemical reservoirs subject to external work and entropy changes. Such a theory is all the more necessary nowadays, when promising technological applications, such as biomimetics [16,17] and chemical computing [18], are envisaged that deliberately exploit the self-organized structures of RDSs. In this respect, the work needed to manipulate a Turing pattern and the efficiency with which information exchanges through traveling waves can occur are thermodynamic questions of crucial importance.

In this Letter, we lay the basis to address these questions by presenting a rigorous thermodynamic theory of RDSs far from equilibrium. We take the viewpoint of stochastic thermodynamics [19,20] and carry over its systematic way to define thermodynamic quantities (such as work and entropy), anchoring them to the (herein deterministic) dynamics of the RDSs. Stochastic thermodynamics has recently emerged as a comprehensive framework for describing *small* systems arbitrarily far from equilibrium, as it allows one to study the efficiency of thermal microengines [21], rationalize the fluctuation theorems [22], and connect information processing to work [23]. We supplement this well-established approach with a novel yet pivotal element, which is the inclusion of the conservation laws [24–26] of the underlying chemical network (CN) for constructing thermodynamic potentials under general nonequilibrium conditions. Moreover, viewing the RDS as the *large size limit* of stochastically reacting and diffusing chemicals, we can study Turing patterns as instances of thermodynamic nonequilibrium phase transitions [27–32].

Theory.—The description of Ref. [33] is extended to CNs endowed with a spatial structure. We consider a dilute ideal mixture of chemical species σ that diffuse within a vessel $\mathcal{V} \ni \boldsymbol{r}$ with impermeable walls and undergo elementary reactions ρ. The abundance of some species is possibly controlled by the coupling with external chemostats (if not, the system is called closed). Hence, the concentration $Z_\sigma(\boldsymbol{r}, t)$ of internal and chemostatted species, respectively denoted x and y follows the reaction-diffusion equations

$$\partial_t Z_\sigma = -\nabla \cdot \boldsymbol{J}_\sigma + \sum_\rho \mathbb{S}_\rho^\sigma j_\rho + I_\sigma. \tag{1}$$

Fick's diffusion currents $\boldsymbol{J}_\sigma = -D_\sigma \nabla Z_\sigma$ are responsible for the transport of chemicals across space and vanish at the boundaries of $\mathcal{V}$; the external currents $I_\sigma \neq 0 \,\forall\, y$ describe the rate at which the controlled species are injected into the (open) system by the chemostats; $\mathbb{S}^\sigma_\rho j_\rho$ gives the concentration variation upon reaction ρ. Here, $\mathbb{S}^\sigma_\rho = \nu^\sigma_{-\rho} - \nu^\sigma_{+\rho}$ is the stoichiometric matrix, i.e., the negative difference between the number of species σ involved in the forward $(+\rho)$ and backward $(-\rho)$ reaction and $j_\rho = j_{+\rho} - j_{-\rho}$ is the net reaction current. While the former specifies the CN topology, the latter determines its kinetics. By virtue of the mass-action kinetics assumption [34], each reaction current is proportional to the product of the reacting species concentrations, $j_{\pm\rho} = k_{\pm\rho}\prod_\sigma Z_\sigma^{\nu^\sigma_{\pm\rho}}$. For example, the net current associated with the autocatalytic reaction $2X_1 + X_2 \underset{k_-}{\overset{k_+}{\rightleftharpoons}} 3X_1$ (the core of the Brusselator model discussed later) is $j_\rho = k_+ Z^2_{X_1} Z_{X_2} - k_- Z^3_{X_1}$, where $\nu^{X_1}_{+\rho} = 2$, $\nu^{X_2}_{+\rho} = 1$, and $\nu^{X_1}_{-\rho} = 3$. Thermodynamic equilibrium characterized by homogeneous concentrations Z^{eq}_σ is reached when all external and reaction currents vanish identically, $j_\rho = I_\sigma = 0$. It implies for the rate constants the *local detailed balance* condition $k_{+\rho}/k_{-\rho} = \prod_\sigma (Z^{\mathrm{eq}}_\sigma)^{\mathbb{S}^\sigma_\rho}$. Such a relation is taken to be valid irrespective of the system's state. The CN instead may be in a *global* nonequilibrium state characterized by space-dependent concentrations $Z_\sigma(\boldsymbol{r}, t)$ as a result of inhomogeneous initial conditions or because of nonvanishing external currents I_σ. Yet, we assume it to be kept by the solvent in *local* thermal equilibrium at a given temperature T. Therefore, the species can be assigned thermodynamic state functions, which have the known equilibrium form valid for dilute ideal mixtures but are a function of the nonequilibrium concentrations $Z_\sigma(\boldsymbol{r}, t)$ (Ref. [35], Chap. 15).

A central role is played by the nonequilibrium chemical potential $\mu_\sigma(\boldsymbol{r}) \coloneqq \mu^\circ_\sigma + \ln Z_\sigma(\boldsymbol{r})$ (given in units of temperature T times the gas constant R, as any other quantity hereafter). It renders the local detailed balance in the form $k_{+\rho}/k_{-\rho} = \exp(-\sum_\sigma \mathbb{S}^\sigma_\rho \mu^\circ_\sigma)$ involving only the difference between the energy of formation of reactants and products. Moreover, its variation across space and between species gives the local diffusion and reaction affinity [34]

$$\boldsymbol{F}_\sigma(\boldsymbol{r}) \coloneqq -\nabla\mu_\sigma(\boldsymbol{r}), \qquad f_\rho(\boldsymbol{r}) \coloneqq -\sum_\sigma \mathbb{S}^\sigma_\rho \mu_\sigma(\boldsymbol{r}), \tag{2}$$

which are the thermodynamic forces driving the system.

We introduce as nonequilibrium potential the "canonical" Gibbs free energy of the system $G \coloneqq \int_{\mathcal{V}} d\boldsymbol{r} \sum_\sigma (\mu_\sigma Z_\sigma - Z_\sigma)$ (given up to a constant). It can be expressed in terms of the equilibrium free energy $G^{\mathrm{eq}} = G(Z^{\mathrm{eq}}_\sigma)$ as

$$G = G^{\mathrm{eq}} + \mathcal{L}(Z_\sigma \| Z^{\mathrm{eq}}_\sigma) \tag{3}$$

introducing the *relative entropy* for non-normalized concentration distributions

$$\mathcal{L}(Z_\sigma \| Z^{\mathrm{eq}}_\sigma) \coloneqq \int_{\mathcal{V}} d\boldsymbol{r} \sum_\sigma \left(Z_\sigma \ln \frac{Z_\sigma}{Z^{\mathrm{eq}}_\sigma} - (Z_\sigma - Z^{\mathrm{eq}}_\sigma) \right). \tag{4}$$

Akin to the Kullback–Leibler divergence for probability densities [36], Eq. (4) quantifies the dissimilarity between two concentrations: Being positive for all $Z_\sigma \neq Z^{\mathrm{eq}}_\sigma$, it implies that G is always larger than its equilibrium counterpart G^{eq}. Most importantly, it is minimized by the relaxation dynamics of *closed* systems. This is shown by evaluating the time derivative of Eq. (3) with the aid of Eq. (1) at $I_\sigma = 0$ and Eq. (2),

$$d_t\mathcal{L} = d_t G = -\dot{\Sigma}_{\mathrm{dff}} - \dot{\Sigma}_{\mathrm{rct}} \eqqcolon -\dot{\Sigma} \leq 0, \tag{5}$$

and recognizing the standard form of the total entropy production rate (EPR) $\dot{\Sigma}$ split into its diffusion and reaction parts [34]:

$$\dot{\Sigma}_{\mathrm{dff}} \coloneqq \int_{\mathcal{V}} d\boldsymbol{r} \sum_\sigma \mathbf{J}_\sigma \cdot \mathbf{F}_\sigma, \qquad \dot{\Sigma}_{\mathrm{rct}} \coloneqq \int_{\mathcal{V}} d\boldsymbol{r} \sum_\rho j_\rho f_\rho. \tag{6}$$

The relative entropy (4) possesses some important physical features. First, in the absence of reactions, it gives the total entropy produced by the diffusive expansion of concentrations. For example, consider n_A and n_B moles of inert chemicals A and B initially placed in the volume fractions V_A and V_B, respectively. They relax to homogeneous concentrations with an entropy production $-\mathcal{L} = n_A \log V_A + n_B \log V_B$ that is exactly the *entropy of mixing* of the two species [37]. It is remarkable that diffusive dissipation and mixing entropy are, thus, fully described in a purely information theoretic fashion, namely, as a relative entropy between concentrations. Second, the relative entropy between reacting concentrations $Z_\sigma(\boldsymbol{r}, t) = \bar{Z}_\sigma(t)\phi_\sigma(\boldsymbol{r}, t)\mathcal{V}$ and arbitrary reference homogeneous concentrations Z^h_σ can be split into the relative entropy between space-averaged concentrations $\bar{Z}_\sigma(t) = \int_{\mathcal{V}} d\boldsymbol{r} Z_\sigma(\boldsymbol{r}, t)/\mathcal{V}$ and equilibrium ones Z^{eq}_σ plus the relative entropy of the normalized local modulations $\phi_\sigma(\boldsymbol{r})$ around $\bar{Z}_\sigma$ and the flat distribution $1/\mathcal{V}$:

$$\mathcal{L}(Z_\sigma \| Z^h_\sigma) = \mathcal{L}(\bar{Z}_\sigma \| Z^h_\sigma) + \sum_\sigma \bar{Z}_\sigma \mathcal{L}(\phi_\sigma \| 1/\mathcal{V}). \tag{7}$$

The positivity of relative entropy implies $\mathcal{L}(Z_\sigma \| Z^h_\sigma) \geq \mathcal{L}(\bar{Z}_\sigma \| Z^h_\sigma)$; i.e., the free energy of a patterned system is always larger than its homogeneous counterpart. Third, different patterns may have the same relative entropy (see Fig. 1) indicating that morphology and thermodynamics need not be correlated [38].

The conservation laws of the CN play a central role in building the nonequilibrium thermodynamics of the system, i.e., in the derivation of Eqs. (3) and (4). The left null vectors of $\mathbb{S}^\sigma_\rho$, i.e., $\sum_\sigma \ell^\lambda_\sigma \mathbb{S}^\sigma_\rho = 0$, define the components

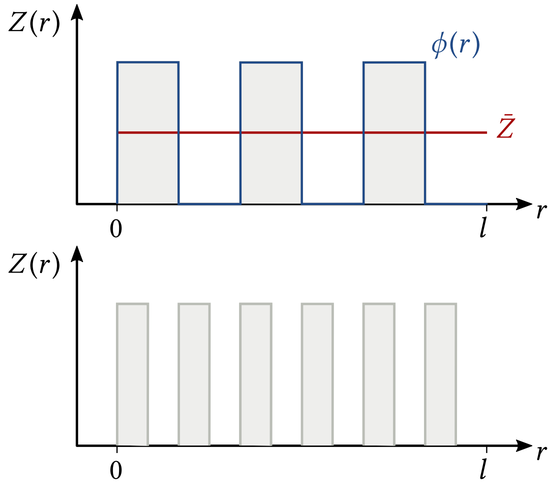

FIG. 1. Sketch of two patterns with equal relative entropy. Any transformation $\phi(r) \to \phi'(r) = \phi(r')$ with $|\partial r/\partial r'| = 1$ corresponding to a simple rearrangement of the local concentrations leaves $\mathcal{L}(Z|Z^{\text{eq}})$ unchanged. This is rooted in the lack of interactions between chemicals at the scale of the RDS.

$L_\lambda = \sum_\sigma \ell^\lambda_\sigma Z_\sigma$, which are the global conserved quantities of the closed system: $d_t \int_\mathcal{V} d\boldsymbol{r} L_\lambda = 0$. For this reason, ℓ^λ_σ are called conservation laws. Physically, they identify parts of molecules called moieties exchanged between species [39]. When the system is opened by chemostatting, ℓ^λ_σ differentiate into the $\ell^{\lambda_u}_\sigma$'s that are left null vectors of the submatrix of internal species $\mathbb{S}^x_\rho$ and the $\ell^{\lambda_b}_\sigma$'s that are not, namely,

$$\sum_x \ell^{\lambda_u}_x \mathbb{S}^x_\rho = 0, \qquad \sum_x \ell^{\lambda_b}_x \mathbb{S}^x_\rho \neq 0. \tag{8}$$

Accordingly, the unbroken components $L_{\lambda_u} = \sum_\sigma \ell^{\lambda_u}_\sigma Z_\sigma$ remain global conserved quantities of the system, $d_t \int_\mathcal{V} d\boldsymbol{r} L_{\lambda_u} = 0$, while the broken ones $L_{\lambda_b} = \sum_\sigma \ell^{\lambda_b}_\sigma Z_\sigma$ change over time, $d_t \int_\mathcal{V} d\boldsymbol{r} L_{\lambda_b} = \sum_y \ell^{\lambda_b}_y \int_\mathcal{V} d\boldsymbol{r} I_y \neq 0$.

In light of that, the equilibrium condition $\sum_\sigma \mathbb{S}^\sigma_\rho \mu^{\text{eq}}_\sigma = 0$ corresponding to null reaction affinities $f_\rho = 0$ implies that μ^{eq}_σ is a linear combination of the conservation laws ℓ^λ_σ. This entails $\int_\mathcal{V} d\boldsymbol{r} \sum_\sigma \mu^{\text{eq}}_\sigma \partial_t Z_\sigma = 0$, which yields, in turn, the decomposition (3) when time integrating along a relaxation dynamics that leads from Z_σ to Z^{eq}_σ [40].

Moreover, the conservation laws are the passkey to construct the correct nonequilibrium thermodynamic potential for *open* systems. For the latter, an additional term appears when taking the time derivative of G due to the external current in Eq. (1),

$$\dot{W}_{\text{chem}} := \int_\mathcal{V} d\boldsymbol{r} \sum_y \mu_y(\boldsymbol{r}) I_y(\boldsymbol{r}), \tag{9}$$

which defines the chemical work performed by the chemostats. The second law (5) thus attains the new form

$$\dot{W}_{\text{chem}} - d_t G = \dot{\Sigma} \geq 0, \tag{10}$$

where the EPR $\dot{\Sigma}$ is still given by the two contributions of Eq. (6) even for $I_\sigma \neq 0$. Consequently, G is no longer minimized due to the break of conservations laws. Similar to equilibrium thermodynamics when passing from canonical to grand canonical ensembles, one needs to transform the free-energy G subtracting the energetic contributions of matter exchanged with the reservoirs [41]. This amounts to the moieties of the broken components $M_{y_p} := \sum_{\lambda_b} \ell^{\lambda_b\,-1}_{y_p} \int d\boldsymbol{r} L_{\lambda_b}(\boldsymbol{r})$ entering those chemostats y_p that break all conservation laws, times the reference values of their chemical potential $\mu^{\text{ref}}_{y_p}$ (which simplifies to μ_{y_p} for homogeneous chemostats). The so-obtained semigrand Gibbs free energy

$$\mathcal{G} := G - \sum_{y_p} \mu^{\text{ref}}_{y_p} M_{y_p} \tag{11}$$

encodes CN-specific topological and spatial features thanks to the freedom in the choice of y_p and $\mu^{\text{ref}}_{y_p}$. This allows one to split the EPR

$$\dot{W}_{\text{driv}} + \dot{W}_{\text{nc}} - d_t \mathcal{G} = \dot{\Sigma}, \tag{12}$$

in terms of the driving and the nonconservative chemical work rate, respectively,

$$\dot{W}_{\text{driv}} := -\sum_{y_p} d_t \mu^{\text{ref}}_{y_p} M_{y_p}, \quad \dot{W}_{\text{nc}} := \sum_y \int_\mathcal{V} d\boldsymbol{r} I_y \mathcal{F}_y. \tag{13}$$

The former results from time-dependent manipulations of the reference chemostats y_p, while the latter gives the cost of sustaining chemical flows by means of the forces $\mathcal{F}_y(\boldsymbol{r}) = \mu_y(\boldsymbol{r}) - \sum_{y_p} \mu^{\text{ref}}_{y_p} \sum_{\lambda_b} \ell^{\lambda_b\,-1}_{y_p} \ell^{\lambda_b}_y$ measured with respect to the reference chemical potentials $\mu^{\text{ref}}_{y_p}$ [40]. Equation (12) is a major result of this Letter and can be verified by direct substitution. It quantifies exactly the energy needed to manipulate, sustain, and create chemical patterns. In the absence of driving ($d_t \mu^{\text{ref}}_{y_p} = 0$) and nonconservative forcing ($\mathcal{F}_y = 0$), it simplifies to $d_t \mathcal{G} = -\dot{\Sigma} \leq 0$, which proves that the CN, despite being *open*, relaxes to equilibrium by minimizing the free energy $\mathcal{G}$. Moreover, for a generic open CN, the decomposition of $\mathcal{G}$ corresponding to Eq. (3), i.e., $\mathcal{G} - \mathcal{G}^{\text{eq}} = \mathcal{L}(Z_\sigma \| Z^{\text{eq}}_\sigma) \geq 0$, and a time integral between two nonequilibrium states connected by an arbitrary manipulation turn Eq. (12) into a *nonequilibrium Landauer principle* [36] for RDS,

$$W_{\mathrm{driv}} + W_{\mathrm{nc}} - \Delta\mathcal{G}_{\mathrm{eq}} \geq \Delta\mathcal{L}(Z_\sigma \| Z_\sigma^{\mathrm{eq}}). \tag{14}$$

The latter states that the dissipative work spent to manipulate the CN is bounded by the variation in relative entropy between the boundary states and their respective equilibria attained by stopping the driving and zeroing the forcing.

Turing pattern in the Brusselator model.—As first proposed by Turing in his seminal paper [42], RDSs undergo a spatial symmetry breaking leading to a stationary pattern when at least two chemical species react nonlinearly and their diffusivities differ substantially. A minimal system that captures these essential features is the Brusselator model [43] in one spatial dimension. Here, the concentrations of two chemical species, an activator $Z_{X_1} = x_1(r,t)$ and an inhibitor $Z_{X_2} = x_2(r,t)$, evolve in time and space $r \in [0, l]$ according to the RDS (1) for the chemical equations in Fig. 2, namely,

$$\partial_t \begin{pmatrix} x_1 \\ x_2 \end{pmatrix} = \underbrace{\begin{pmatrix} k_1 y_1 - k_{-1} x_1 - k_2 y_2 x_1 + k_{-2} y_3 x_2 + k_3 x_1^2 x_2 - k_{-3} x_1^3 - k_4 x_1 + k_{-4} y_4 + D_{x_1} \partial_r^2 x_1, \\ k_2 y_2 x_1 - k_{-2} y_3 x_2 - k_3 x_1^2 x_2 + k_{-3} x_1^3 + D_{x_2} \partial_r^2 x_2 \end{pmatrix}}_{=\mathcal{J}(x_1, x_2)}. \tag{15}$$

The y_1, y_2, y_3, and y_4 are the homogeneous concentrations of the chemostatted species, and the diffusivities satisfy the Turing condition $D_{x_1} \ll D_{x_2}$. Equation (15) admits a homogeneous stationary solution $(x_1^h, x_2^h)^\intercal$ that becomes unstable for $y_2 \geq y_2^c$ so that a sinusoidal pattern with wave number q_c and amplitude proportional to the (in general complex) function $A(r,t)$ starts developing around the space-averaged concentrations $\bar{x}(t)$ [35]:

$$\begin{pmatrix} x_1(r,t) \\ x_2(r,t) \end{pmatrix} = \begin{pmatrix} \bar{x}_1(t) \\ \bar{x}_2(t) \end{pmatrix} + \begin{pmatrix} 1 \\ u_{x_2} \end{pmatrix} [A(r,t) e^{i q_c r} + \mathrm{c.c.}]. \tag{16}$$

The critical values y_2^c and q_c are determined by the condition of marginal stability of the homogeneous state: They are the smaller values for which the matrix $\partial_x \mathcal{J}(x_1^h, x_2^h)$ (evolving linearized perturbations) acquires a zero eigenvalue, the corresponding eigenvector being $(1, u_{x_2})^\intercal$. Near the onset of instability, one can treat $\epsilon = (y_2 - y_2^c)/y_2^c \ll 1$ as a small parameter and carry out a perturbation expansion in powers of ϵ. This leads to the amplitude equation for $A(r,t)$ [44],

$$\tau \partial_t A = \epsilon A - \alpha |A|^2 A + \xi \partial_r^2 A, \tag{17}$$

which describes an exponential growth from an initial small perturbation $A(r,0) \simeq 0$ followed by a late-time saturation due to the nonlinear terms in Eq. (15). Amplitude equations provide a general quantitative description of pattern formation in several systems near the onset of instability [45], irrespective of the details of the underlying physical process that is subsumed into the effective coefficients τ, α, and ξ. Since Eq. (17) can be seen as a gradient flow in a complex Ginzburg-Landau potential involving a bifurcation as ϵ turns positive, pattern formation is usually considered a *dynamical* phase transition [46]. Here, using an analytical approximate solution to Eq. (15) valid for $\epsilon \ll 1$, we show that the phenomenon is, in fact, a genuine *thermodynamic* phase transition identified by the appearance of a kink singularity at y_2^c in the nonequilibrium free energy $\mathcal{G}(y_2)$. The semigrand canonical free energy of Fig. 2 is calculated [40] taking the stationary stable solution corresponding to a given value of y_2, i.e., the homogenous one for $y_2 \leq y_2^c$ and the patterned one for $y_2 > y_2^c$, namely,

$$\begin{pmatrix} x_1^p(r) \\ x_2^p(r) \end{pmatrix} \sim \begin{pmatrix} 1 \\ u_{x_2} \end{pmatrix} \sqrt{\frac{\epsilon}{\alpha}} 2 \cos(q_c r). \tag{18}$$

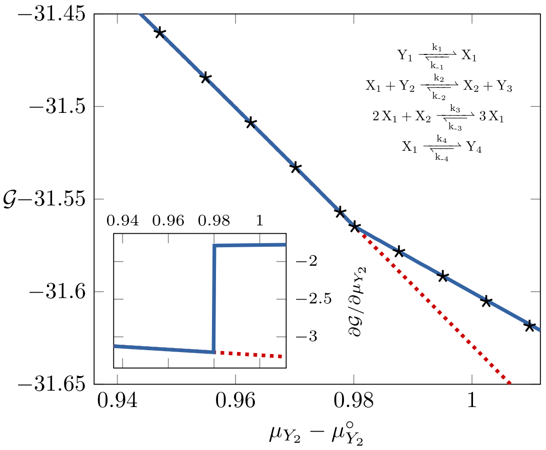

FIG. 2. Nonequilibrium semigrand Gibbs free energy $\mathcal{G}$ for the Brusselator model as a function of the chemical potential of the chemostatted species Z_{Y_2} obtained by the analytic stationary solution of the amplitude equation. To define $\mathcal{G}$, we choose y_1 and y_2 as the reference chemostats breaking the two components $L_1 = x_1 + x_2 + y_1 + y_4$ and $L_2 = y_2 + y_3$. The dotted line represents the free energy $\mathcal{G}$ in the unstable homogeneous system before the pattern growth. Symbols ($\star$) result from numerical integration of Eq. (15). Inset: The derivative $\partial\mathcal{G}/\partial\mu_{Y_2}$ displays a discontinuity at $y_2^c \simeq 2.66$.

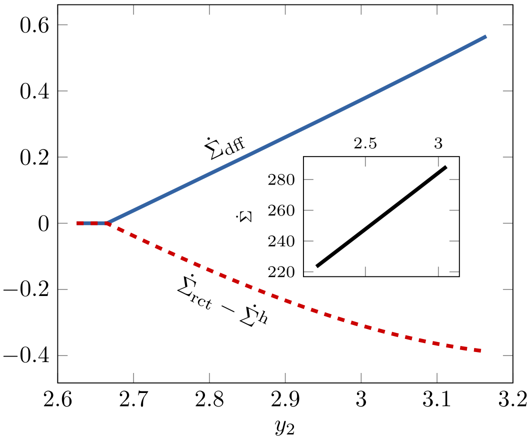

FIG. 3. Analytical result for the EPR of reaction $\dot{\Sigma}_{\mathrm{rct}}$ (dashed) and diffusion $\dot{\Sigma}_{\mathrm{dff}}$ (solid) in the stable stationary state as function of the concentration y_2. The EPR of the (unstable for $y_2 > y_2^c$) homogeneous state $\dot{\Sigma}^h$ is subtracted from the former to show the effect of the pattern formation, i.e., decreasing reaction dissipation at the expense of diffusion dissipation. Inset: The total entropy production shows no singularity at the phase transition. All results correspond to the weakly reversible case $k_{-\rho} = 10^{-4} \ll k_{+\rho} = 1$, and $y_3 = y_4 = 10^{-4}$, $y_1 = 2$, $D_{x_1} = 1$, $D_{x_2} = 10$.

The physical meaning of the kink at $y_2 = y_2^c$ is best understood noticing that the quantity $\partial \mathcal{G}/\partial \mu_{Y_2} = \dot{W}_{\mathrm{driv}}/d_t \mu_{Y_2}$ is the driving work upon a quasistatic manipulation of the chemical potential μ_{Y_2}. In particular, for $y_2 > y_2^c$ it represents the minimum work needed to vary the wave number q_c of the Turing pattern [18]. Interestingly, the total EPR shows no singularity at the transition (cf. Fig. 3): Moving across y_2^c, the EPR of reaction $\dot{\Sigma}_{\mathrm{rct}}$ decreases with respect to the homogeneous state value $\dot{\Sigma}^h$, while a nonzero EPR of diffusion appears, their sum being continuous. This is different from what has been observed in some previous studies of nonequilibrium phase transition [27–31].

Conclusion.—We presented the nonequilibrium thermodynamics of RDSs and exemplified the theory with the application to the Brusselator model. We went beyond the conventional treatment of classical nonequilibrium thermodynamics [47] in two respects: avoiding to linearize the chemistry, i.e., to oversimplify reaction affinities to currents times Onsager coefficients; explicitly building thermodynamic potentials that act as Lyapunov functions in the relaxation to equilibrium provide minimum work principles and reveal the existence of nonequilibrium phase transitions. As demonstrated by the paradigmatic case of the Brusselator model, the framework can be directly applied to quantify the energy cost of pattern manipulations in complex biochemical systems [48–50] and paves the way to study information transmission in signal transduction [51], quorum sensing [52], and chemotaxis [53].

We acknowledge funding from the National Research Fund of Luxembourg (AFR Ph.D. Grant 2014-2, No. 9114110) and the European Research Council project NanoThermo (ERC-2015-CoG Agreement No. 681456).

[1] V. Castets, E. Dulos, J. Boissonade, and P. De Kepper, Phys. Rev. Lett. **64**, 2953 (1990).
[2] Q. Ouyang and H. L. Swinney, Nature (London) **352**, 610 (1991).
[3] A. N. Zaikin and A. M. Zhabotinsky, Nature (London) **225**, 535 (1970).
[4] A. T. Winfree, Science **175**, 634 (1972).
[5] P. J. Ortoleva, *Geochemical Self-Organization* (Oxford University Press, New York, 1994).
[6] J. D. Murray, *Mathematical Biology. II Spatial Models and Biomedical Applications*, 3rd ed. (Springer-Verlag, Berlin 2001).
[7] S. Kondo and T. Miura, Science **329**, 1616 (2010).
[8] D. Iber and D. Menshykau, Open Biol. **3**, 130088 (2013).
[9] S. Kretschmer and P. Schwille, Curr. Opin. Cell Biol. **38**, 52 (2016).
[10] M. Falcke, Adv. Phys. **53**, 255 (2004).
[11] K. Thurley, A. Skupin, R. Thul, and M. Falcke, Biochim. Biophys. Acta **1820**, 1185 (2012).
[12] I. Prigogine and G. Nicolis, Q. Rev. Biophys. **4**, 107 (1971).
[13] G. Nicolis and I. Prigogine, *Self-Organization in Nonequilibrium Systems: From Dissipative Structures to Order Through Fluctuations* (Wiley-Blackwell, New York, 1977).
[14] M. C. Cross and P. C. Hohenberg, Rev. Mod. Phys. **65**, 851 (1993).
[15] J. Ross, *Thermodynamics and Fluctuations Far from Equilibrium* (Springer, New York, 2008), Chap. 5.
[16] F. Rossi, S. Ristori, M. Rustici, N. Marchettini, and E. Tiezzi, J. Theor. Biol. **255**, 404 (2008).
[17] B. A. Grzybowski and W. T. Huck, Nat. Nanotechnol. **11**, 585 (2016).
[18] A. Adamatzky, B. De Lacy Costello, and T. Asai, *Reaction-Diffusion Computers* (Elsevier, New York, 2005).
[19] C. Jarzynski, Annu. Rev. Condens. Matter Phys. **2**, 329 (2011).
[20] C. Van den Broeck and M. Esposito, Physica (Amsterdam) **418A**, 6 (2015).
[21] G. Verley, M. Esposito, T. Willaert, and C. Van den Broeck, Nat. Commun. **5**, 4721 (2014).
[22] U. Seifert, Rep. Prog. Phys. **75**, 126001 (2012).
[23] J. M. R. Parrondo, J. M. Horowitz, and T. Sagawa, Nat. Phys. **11**, 131 (2015).
[24] M. Polettini and M. Esposito, J. Chem. Phys. **141**, 024117 (2014).
[25] M. Polettini, G. Bulnes-Cuetara, and M. Esposito, Phys. Rev. E **94**, 052117 (2016).
[26] R. Rao and M. Esposito, New J. Phys. **20**, 023007 (2018).
[27] P. Gaspard, J. Chem. Phys. **120**, 8898 (2004).
[28] T. Tomé and M. J. de Oliveira, Phys. Rev. Lett. **108**, 020601 (2012).
[29] Y. Zhang and A. C. Barato, J. Stat. Mech. (2016) 113207.
[30] E. Crosato, R. E. Spinney, R. Nigmatullin, J. T. Lizier, and M. Prokopenko, Phys. Rev. E **97**, 012120 (2018).

[31] H. Vroylandt, M. Esposito, and G. Verley, Europhys. Lett. **120**, 30009 (2018).

[32] T. Herpich, J. Thingna, and M. Esposito, arXiv:1802.00461 [Phys. Rev. X (to be published)].

[33] R. Rao and M. Esposito, Phys. Rev. X **6**, 041064 (2016).

[34] S. R. de Groot and P. Mazur, *Non-Equilibrium Thermodynamics* (Dover, New York, 1984).

[35] D. Kondepudi and I. Prigogine, *Modern Thermodynamics: From Heat Engines to Dissipative Structures*, 2nd ed. (Wiley, New York, 2014).

[36] M. Esposito and C. Van den Broeck, Europhys. Lett. **95**, 40004 (2011).

[37] A. Ben-Naim, *A Farewell to Entropy: Statistical Thermodynamics Based on Information* (World Scientific Publishing Company, Singapore, 2008), Chap. 6.

[38] H. Serna, A. P. Muñuzuri, and D. Barragán, Phys. Chem. Chem. Phys. **19**, 14401 (2017).

[39] H. S. Haraldsdóttir and R. M. T. Fleming, PLoS Comput. Biol. **12**, e1004999 (2016).

[40] See Supplemental Material at http://link.aps.org/supplemental/10.1103/PhysRevLett.121.108301 for details on mathematical demonstrations.

[41] R. A. Alberty, *Thermodynamics of Biochemical Reactions* (Wiley-Interscience, New York, 2003).

[42] A. Turing, Bull. Math. Biol. **52**, 153 (1990).

[43] I. Prigogine and R. Lefever, J. Chem. Phys. **48**, 1695 (1968).

[44] B. Peña and C. Pérez-García, Phys. Rev. E **64**, 056213 (2001).

[45] M. Cross and H. Greenside, *Pattern Formation and Dynamics in Nonequilibrium Systems* (Cambridge University Press, Cambridge, England, 2009).

[46] I. S. Aranson and L. Kramer, Rev. Mod. Phys. **74**, 99 (2002).

[47] S. Kjelstrup and D. Bedeaux, *Non-Equilibrium Thermodynamics of Heterogeneous Systems*, Vol. 16, (World Scientific, Singapore, 2008).

[48] A. S. Zadorin, Y. Rondelez, J.-C. Galas, and A. Estevez-Torres, Phys. Rev. Lett. **114**, 068301 (2015).

[49] I. R. Epstein and B. Xu, Nat. Nanotechnol. **11**, 312 (2016).

[50] J. Halatek and E. Frey, Nat. Phys. **14**, 507 (2018).

[51] S. Ito and T. Sagawa, Nat. Commun. **6**, 7498 (2015).

[52] A. F. Taylor, M. R. Tinsley, F. Wang, Z. Huang, and K. Showalter, Science **323**, 614 (2009).

[53] G. Micali and R. G. Endres, Curr. Opin. Microbiol. **30**, 8 (2016).